CORROSION RESISTANCE OF AUSTENITIC AND SUPERAUSTENITIC STAINLESS STEEL IN SYNTHETIC OIL FIELD FORMATION WATER MEASURED BY STEP POTENTIAL *

João Matheus Batista Amaro de Sousa[1]
Jorge Luiz Cardoso[2]
Pedro de Lima Neto[3]
Marcelo José Gomes da Silva[4]

Abstract

The pre-salt region is very hostile to the materials used in such environment due to some factors found under the pre-salt layer such as: corrosive gases, oil formation water, high pressures and so on. In order to evaluate only the effect of the oil field formation water on the corrosion resistance of austenitic stainless steels in such environment, two austenitic and two superaustenitic stainless steels were tested in synthetic oil field formation water using the electrochemical technique called step potential. In this technique, potential values (vs Ag/AgCl) is applied in steps of 50 mV every 1 h until a current of 1 mA was achieved. The results showed that the common austenitic stainless steels are not suitable for the use in chloride-containing environment as the one found in the pre-salt region. They exhibited pitting corrosion. The superaustenitic stainless steels tested exhibited a good corrosion resistance in this medium and can be a solution for the use under some pre-salt conditions.

Keywords: Step potential; Pitting corrosion; Austenitic stainless steels.

[1] *Metallurgical Engineering, undergraduation student, department of metallurgical engineering and materials, Federal University of Ceará, Fortaleza - Brazil.*
[2] *Eng. and Materials Science, doctor, department of metallurgical engineering and materials, Federal University of Ceará, Fortaleza – Brazil.*
[3] *Physicochemical, doctor, department of chemistry, Federal University of Ceará, Fortaleza, Brazil.*
[4] *Nuclear Engineering, doctor, department of metallurgical engineering and materials, Federal University of Ceará, Fortaleza - Brazil.*

** Technical contribution to the 74º Congresso Anual da ABM – Internacional, part of the ABM Week 2019, October 1st-3rd, 2019, São Paulo, SP, Brazil.*

5 **1 INTRODUCTION**

In the pre-salt region, there are two types of technological challenges for the exploration of oil and gas. The vertical challenge that consists in drilling the well as far as the reservoir, crossing water layers, sediment and salt. Each layer with a different behavior at temperatures ranging from 50 °C to 150 °C under high pressures and corrosive gases. The two main corrosive gases found there, carbon dioxide (CO_2) and hydrogen sulfide (H_2S), when in contact with water from these reservoirs accelerate the corrosion of metallic materials used for the oil exploration in the pre-salt region [1]. The way back to the surface must also be considered, once that all the oil and natural gas extracted from the well will be transported through the pipelines and the material from which the pipes are made must resist all adverse conditions to avoid oil leaks. This oil has good quality but never comes alone. It is mixed with oil formation water and the understanding of the effect of this solution on steels is of paramount importance. This is the vertical challenge. The horizontal one consists in the transportation of oil and gas from the production area to the coast localized about 300 km away from the well location [1]. The oil field formation water is expected to have a great amount of NaCl, once this water is found below a salt layer. Thus, pitting corrosion can occur on the steels used for this type pf extraction. Good materials recommended for the use where corrosion can occur is the austenitic stainless steels. In certain environments, especially those containing chloride ions, these steels are susceptible to a form of localized corrosion called pitting corrosion [2, 3]. The addition of alloying elements such as molybdenum has the role of reducing the susceptibility to this form of corrosion, since this element is incorporated into the passive film by the formation of complex oxides in different oxidation states [4]. Cardoso et al. [5] studied the corrosion resistance of four austenitic stainless steels in chloride-containing medium, three of them belonging to the 300 series and the other a superaustenitic one. The authors concluded that the superaustenitic one exhibited a good corrosion resistance while the common austenitic of 300 series exhibited pitting corrosion. The superaustenitic stainless steels can be considered as one of the solution for the problems involving oil extractions in chloride-containing medium.

2 DEVELOPMENT

2.1 Materials

The materials used in this research were the AL-6XN PLUS™ superaustenitic stainless steel provided by the American company Allegheny Ludlum Corporation, the 904L superaustenitic stainless steel provided by the Fluminense Federal University (UFF) and the 300 series austenitic stainless steels AISI 316L and 317L provided by the Federal University of Ceará (UFC). Table 1 presents the chemical composition of the studied steels measured in an Optical Emission Spectrometer (PDA-7000 SHIMADZU).

Table 1. Chemical composition (wt%) of the studied alloys and the respective PRE_N.

Alloys	C	N	Mn	Si	Cr	Ni	Mo	PRE_N
316L	0.030	0.05	1.65	0.41	17.2	10.7	2.2	26
317L	0.024	0.06	1.49	0.40	17.8	12.3	3.5	31
904L	0.027	0.10	0.74	0.66	19.5	24.3	4.5	37
AL-6XN PLUS™	0.021	0.24	0.35	0.32	21.8	25.8	7.6	54

The index that measures the pitting corrosion resistance for the studied alloys are also shown in Table 1. The Pitting Corrosion Resistance can be expressed in terms of some alloying elements such as Cr, Mo and N. This expression is known as PRE_N (Pitting Resistance Equivalent Number) and expresses the ability of the alloy to resist pitting corrosion. In chloride-containing media, the PRE_N of austenitic stainless steels can be expressed by the equation 1 [6].

$$PRE_N = \%Cr + 3.3\%Mo + 30\%N \quad \text{(eq.1)}$$

2.2 Characterization of the samples

Figure 1 depicts the dimension (in mm) and shape of the samples for this measurement. The samples were used in the as received condition. Characterization of the samples were carried out using XRD by Synchroton Light (energy 12 keV) in order to detect the phases present (with exception of the 317L alloy due to a manufactory problem of the probes). A database called Joint Committee for Powder Diffraction Data (JCPDS) belonging to ICDD database (International Centre for Diffraction Data) was used to identify the peaks. These measurements were carried out at the Brazilian Synchrotron Light Laboratory in the city of Campinas-SP in Brazil.

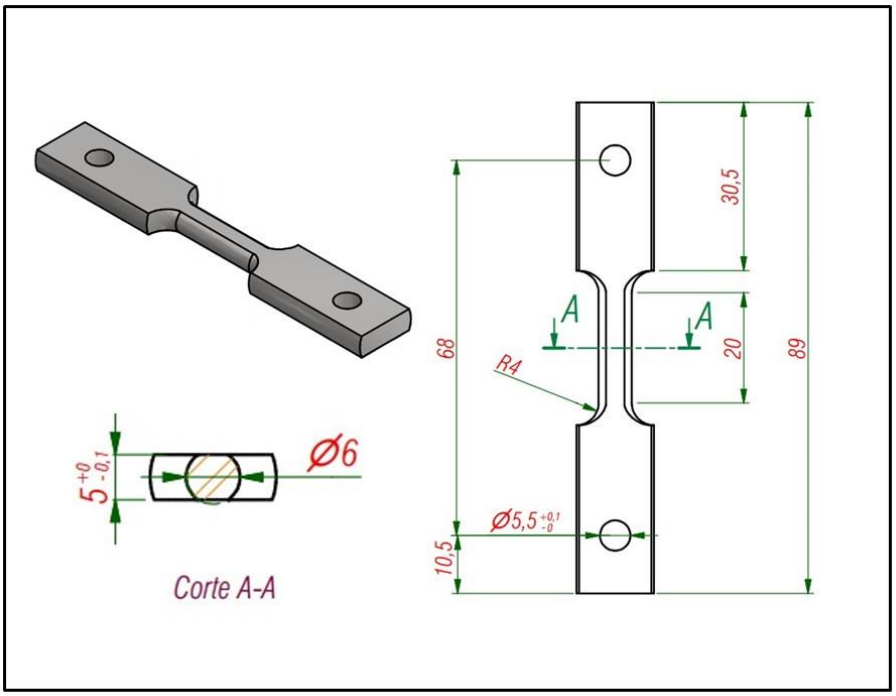

Figure 1. Dimension (in mm) and shape of the samples for the XRD using synchrotron light.

2.3 Electrochemical tests

The electrochemical measurements were carried out at room temperature using the step potential technique. In the preparation for the electrochemical tests, the samples were mounted in cold curing epoxy resin, ground with 600 grade sandpaper, rinsed with ethanol and blow-dried before each measurement. The dimensions of the samples were on average 8.0 mm x 8.0 mm x 3.5 mm. The samples were coated with a lacquer to reduce crevice corrosion on the epoxy/steel edges leaving an exposed area of exactly 1 cm². A three electrode cell configuration was used. A saturated silver/silver-chloride (Ag/AgCl) as reference electrode and a platinum electrode as counter electrode were used. The electrolyte used was a synthetic oil field formation water named by Petrobras of TQ 3219 which composition is shown in Table 2.

Table 2. Chemical composition of the oil field formation water calculated for 1 L of distilled water.

Reagentes	$CaSO_4$	$MgCl_2$	$NaHCO_3$	NaCl	Na_2S
C (g/L)	0.516	4.566	0.425	29	0.072

A potentiostat (AUTOLAB PGSTAT302N) connected to a microcomputer was used. The software NOVA 1.9 was used to obtain data from the step potential curves. Before the measurements, the samples were immersed for 30 min in the solution to determine the open circuit potential (OCP). Subsequently the potential was increased in steps of 50 mV every 1 h until a breakthrough current density was attained. The pitting corrosion initiation potential was defined when the current density reached values above 0.1 mA/cm² [7]. After the tests, the samples were examined by Scanning Electron Microscopy (SEM) to confirm the presence of pits on the alloys surfaces. The tests were carried out in triplicate at room temperature (25°C).

2.4 Results

The phases detected by XRD from Synchroton light are shown in Figure 2. The 2 theta angle was selected in the range of 25 ° to 80 ° in order to detect any deleterious phase like sigma phase. As can be seen in the results, only austenite (FCC) and ferrite peaks (BCC) were observed.

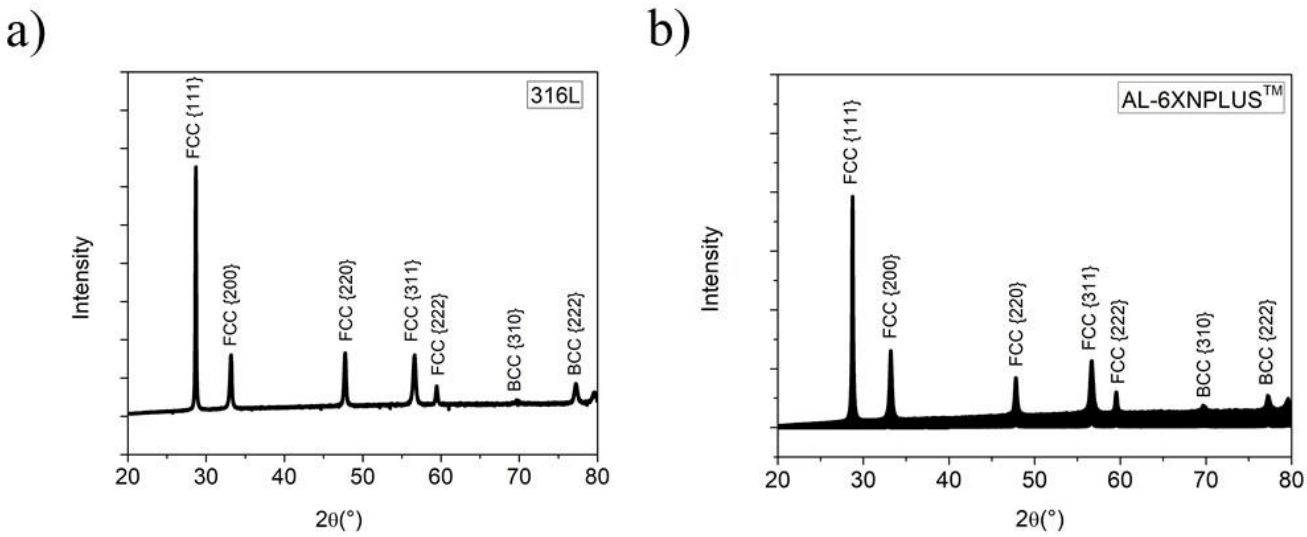

Figure 2. XRD pattern for the (a) 316L steel and (b) AL-6XNPLUS™ in the as received condition (synchrotron light radiation source, λ = 0.10332 nm).

Figure 3 shows the microstructure of the AL-6XN PLUS™ super austenitic stainless steel after an electrolytic etching with oxalic acid 10 %. It is possible to see the grain boundaries and the twin boundaries. This is characteristic of the austenitic phase.

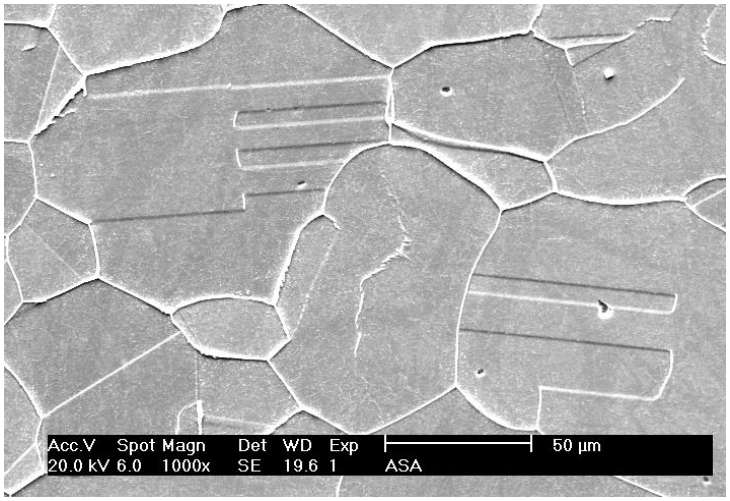

Figure 3. SEM image of the microstructure of the AL-6XN PLUS™ super austenitic stainless steel.

The step potential curves for all the four austenitic stainless steels are shown from Figure 4 to Figure 7. The y-axis is double (potential and current density). As can be

seen, for the common austenitic stainless steels (316L and 317L), the time to achieve the pitting potential is less than the time for the superaustenitic stainless steels (904L and AL-6XNPLUS™).

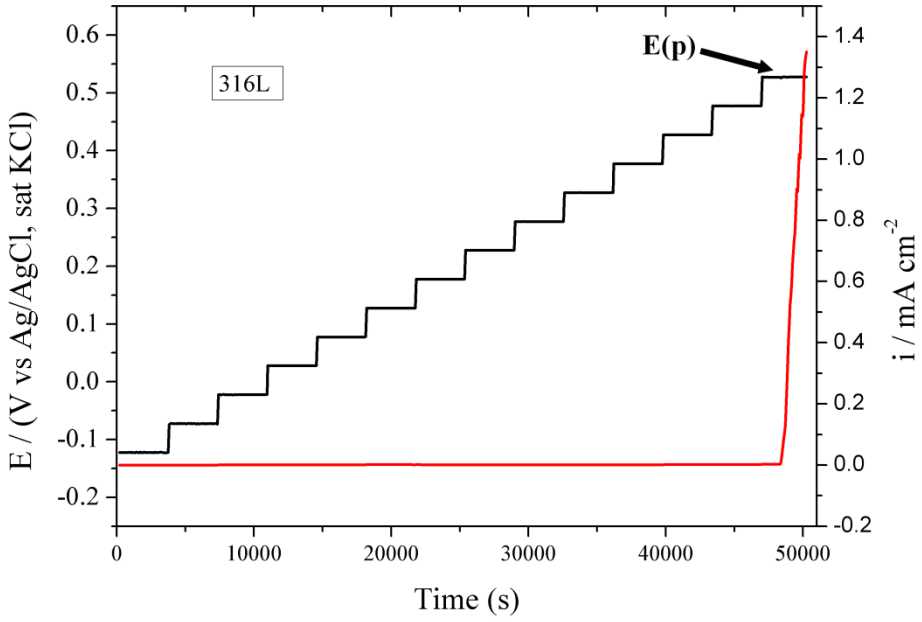

Figure 4. Plot with the step potential curve, the current density and time for the 316L steel in the as received condition.

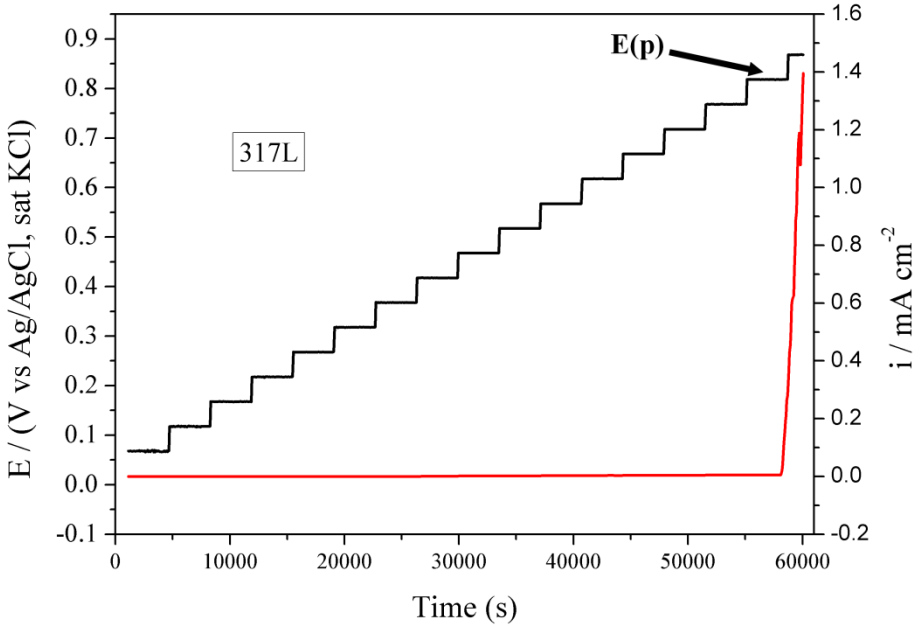

Figure 5. Plot with the step potential curve, the current density and time for the 317L steel in the as received condition.

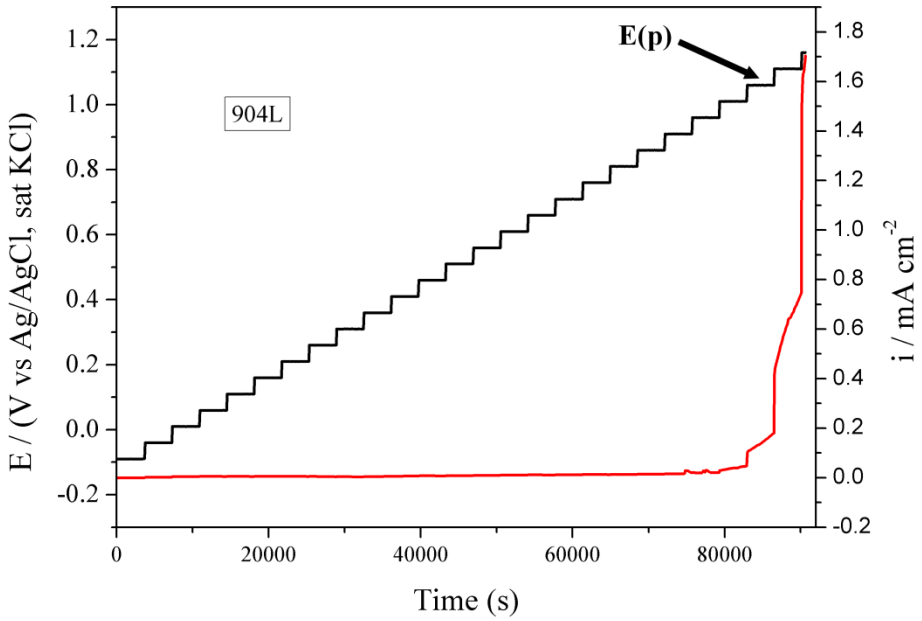

Figure 6. Plot with the step potential curve, the current density and time for the 904L steel in the as received condition.

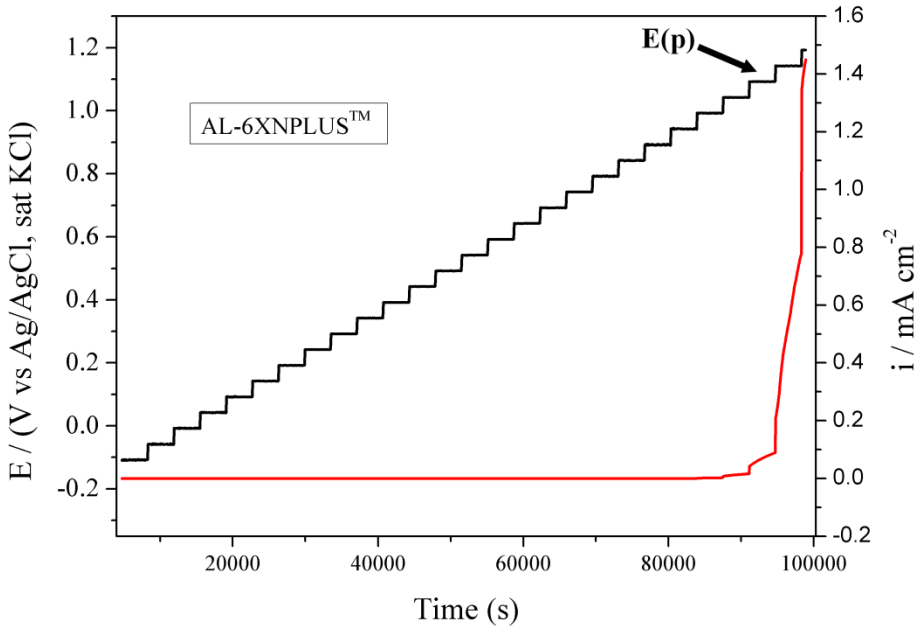

Figure 7. Plot with the step potential curve, the current density and time for the AL-6XNPLUS™ steel in the as received condition.

The pitting corrosion on the common austenitic stainless steels (316L and 317L) can be seen from Figure 8 to Figure 10. The pits grow from inside to outside leaving a deep hole in the center of the pits as can be seen in Figure 9. The superaustenitic ones (904L and AL-6XNPLUS™) did not present pitting corrosion confirming their high corrosion resistance in chloride-containing media.

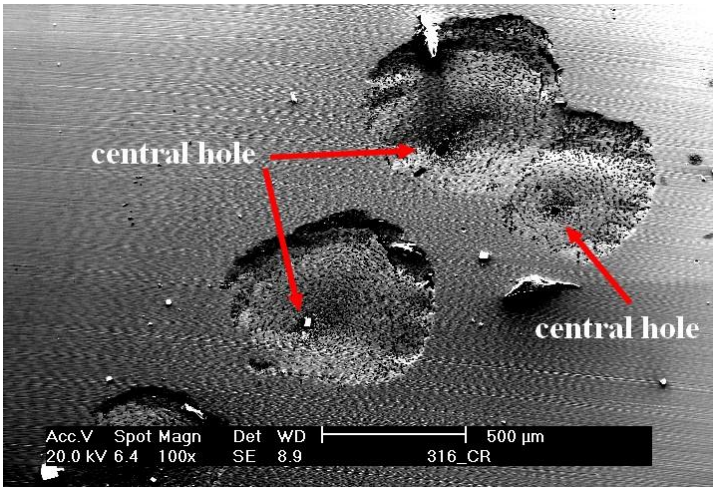

Figure 8. SEM image showing the pits formation on the 316L steel (500 µm).

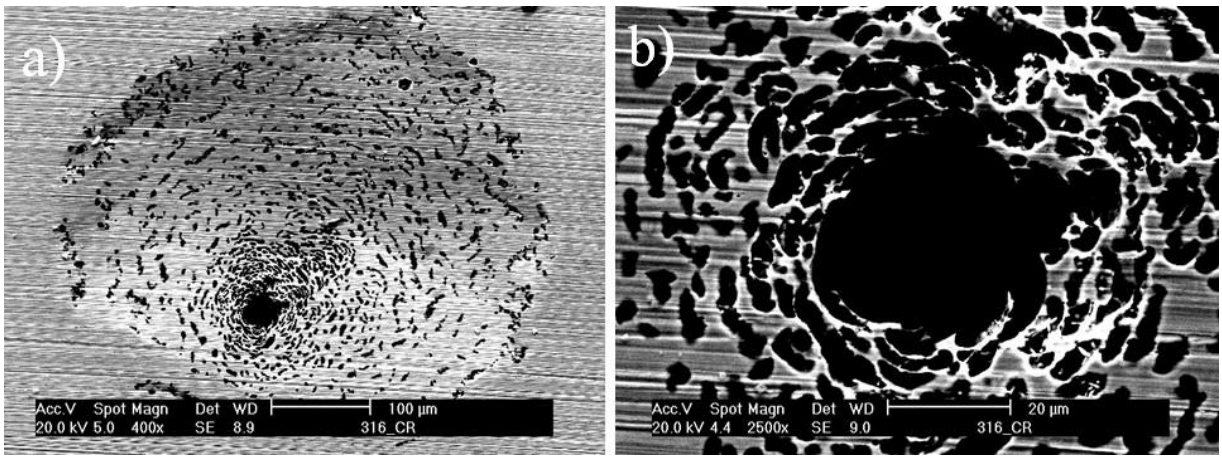

Figure 9. SEM images of the same pit on the 316L steel with different magnitudes, a) 100 µm and b) 20 µm.

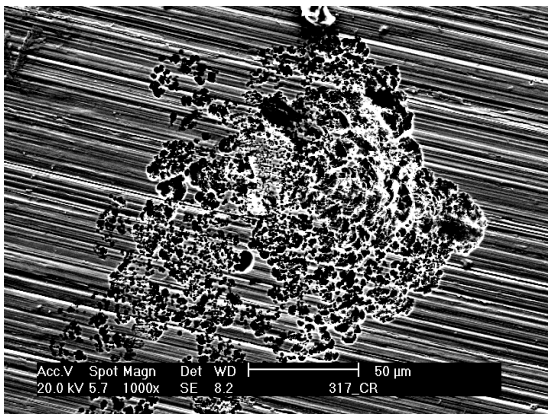

Figure 10. SEM image showing the initiating pits on the 317L steel (50 µm).

Table 3 shows the pitting potential and the necessary time to reach every pitting potential. This time expressed in hour represents the time for the passive film to break.

Table 3. Measured pitting potential of the studied alloys using the Step Potential technique.

Step Potential		
Alloy	E(pit) (V Ag/AgCl)	time (h)
316L	+0.52	13.5
317L	+0.81	16.2
904L	+1.06	23.1
AL-6XN PLUS™	+1.09	26.2

2.5 Discussion

2.5.1 XRD from Synchrotron Light

Austenite peaks (FCC) and some ferrite peaks (BCC) on the diffractogram pattern for the 316L steel were observed as seen in Figure 2a. The same result was found for the AL-6XNPLUS™ steel as can be seen in Figure 2b. The results showed that the two materials are not solution annealed because of the presence of ferrite phase. No sigma phase peak or other phase peaks were detected for this range of 2θ. This means that the results involving reduction of corrosion resistance cannot be attributed to deleterious phases.

2.5.2 Step Potential Curves

From Figure 4 to Figure 8 one can see the results of the step potential in synthetic oil filed formation water. Every potential step is maintained during one hour. If nothing happens on the passive film, then a new step was reached by an increment of 50 mV. The pitting potential (E_p) of each alloy was reached when the current density reached values above 0.1 mA/cm² as shown on the curves. So there is an abrupt increase of the current density indicating the breakdown of the passive film. The time to achieve the pitting potential depends on the film resistance of each alloy. The more resistant the film is, more time is needed to reach the pitting potential. The pitting potential for the 316L steel had the lowest value (0.52 V) while the pitting potential for the 904L and AL-6XNPLUS™ steels had the highest value (1.06 V and 1.09 V, respectively). The pitting potential for the 317L steel had an intermediate value (0.81 V). Table 3 shows the pitting potential and the necessary time to achieve it for each alloy. It was necessary more than one day for the sample of AL-6XNPLUS™ steel to reach its pitting potential. This result shows how resistant is this material. On the other hand, the 316L steel had the lowest time to reach its pitting potential. Even without the presence of CO_2, this steel showed susceptibility to corrosion in chloride-containing environments. The 317L steel showed to be more resistant than the 316L steel in chloride-containing environments but less resistant than the other two super austenitic ones.
The 316L and 317L steels suffered pitting corrosion. Figure 8 shows pits on the 316L surface. The pits have circular shape with a hole in the center. The pitting propagates from the center to the edge and has a tendency to grow with time. This effect is

attributed to the chloride in the solution. The chloride ion (Cl^-) is very small and can penetrate easily in sites of the 316L surface where the film is partially broken. A initiation of non-passivating pits starts (Fig 9a). The pits on the 316L steel grow but only in the center as show in Figure 9b. With the absence of CO_2 in the solution, the environment is not so aggressive to permit the growth of the pits.
The 317L steel also suffered pitting corrosion but its pits are so small when compared to the ones of 316L. The pits initiate but they do not grow with time as shown in Figure 10. It can be seen a non uniform pit. This result indicated that the 317L steel in some chloride-containing environments is also resistant being also a good choice in some applications where the 316L cannot be used, for example, in the oil and gas industry.
The pits formed on the surface of the super austenitic stainless steel (904L and AL-6XNPLUS™) are much smaller than the ones found on the surface of conventional austenitic steels (316L and 317L). They are micro-pits and after initiating, they repassivate before they start to grow. All the micrographs of the alloys taken after the corrosion tests are in accordance with the curves shown before. This experimental procedure has previously been used to qualify Ni-based alloys and hyper duplex stainless steel for raw seawater injection [5]. As explained before, this good resistance is due to the Cr, Mo and Ni content on the composition of the studied alloys relating to PRE_N of each alloy. In some cases, the conventional 317L steel can be also a good option than the conventional 316L steel in chloride-containing environments.

5 CONCLUSION

It can be concluded that the oil field formation water plays an inportant role as as an aggressive substance in the pre-salt region. In chloride-containing environments, the 316L steel is not so resistant and it is not recommended for the content of NaCl in the pre-salt region. The type of corrosion found there was identified as pitting corrosion. The 317L steel presented a good pitting corrosion resistance when compared to the 316L steel. The two superaustenitic stainless steels studied in this research (904L and AL-6XNPLUS™) presented good pitting corrosion resistance and both can be the solution in for applications in in chloride-containing environments as those found in the pre-salt region.

Acknowledgments

The authors would like to thank to Funcap and CAPES for the financial support. A special thank is given to Wilan Italiano, who gave a training in the elechtrochemical tests of step potential and gave also important contributions for this work.

REFERENCES

1 COPPE - INSTITUTO ALBERTO LUIZ COIMBRA DE PÓS-GRADUAÇÃO E PESQUISA DE ENGENHARIA. Race to the sea: the technological and environmental challenges of the pre-salt. Available in:< http://www.coppe.ufrj.br/sites/default/files/coppe_pre-sal.pdf >. (original in Portuguese - access: November 2012).

2 R.L. PAUT et al. A short review on wrought austenitic stainless steel at high temperatures: processing, microestructure, propeties and performance. Materials Research, vol. 10, pp. 453-460, Oct. 2007.

3 SEDRIKS, A.J., Corrosion of Stainless Steels, 2aedição, Nova York: John Wiley & Sons Inc., 1996

4 PADILHA, A. F; RIOS, P. R. Decomposition of austenitic stainless steel. ISIJ International. 325-337, April 2002.

5 Cardoso JL, Nunes Cavalcante ALS, Araújo Vieira RC, Gomes da Silva MJ, de Lima-Neto P. Pitting corrosion resistance of austenitic and superaustenitic stainless steels in aqueous medium of NaCl and H_2SO_4. Journal of Materials Research: 2016; 31: 1755-1763.

6 ALLEGHENY-LUNDLUM. AL-6XN PLUS™ Alloy Technical Data Blue Sheet, 2002.

7 EIDHAGEN. J, KIVISÄKK. U. Crevice corrosion properties for Sandvik SAF 3207™ HD during injection of natural and chlorinated seawater. AB Sandvik Materials Technology, Tube R&D, Sandvik. Eurocorr conference, September 4-8:th, Stockholm, Sweden, 2011.